Journal of Hazardous Materials 397 (2020) 122804

Contents lists available at ScienceDirect

Journal of Hazardous Materials

journal homepage: www.elsevier.com/locate/jhazmat

Ultrasound-assisted heterogeneous activation of persulfate and peroxymonosulfate by asphaltenes for the degradation of BTEX in water

Kirill Fedorov[a], Maksymilian Plata-Gryl[a], Javed Ali Khan[b], Grzegorz Boczkaj[a,*]

[a] Department of Process Engineering and Chemical Technology, Faculty of Chemistry, Gdańsk University of Technology, 80-233, Gdańsk, 11/12 Narutowicza Str., Poland
[b] Radiation Chemistry Laboratory, National Centre of Excellence in Physical Chemistry, University of Peshawar, Peshawar, 25120, Pakistan

GRAPHICAL ABSTRACT

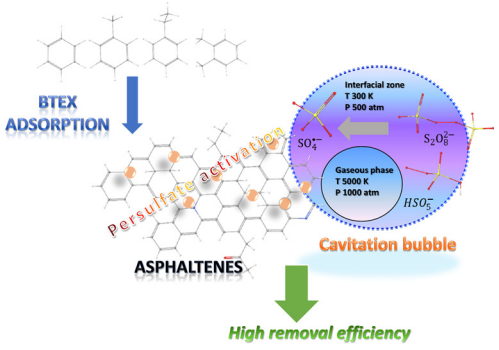

ARTICLE INFO

Keywords:
BTEX
Persulfate
Radicals
Acoustic cavitation
AOPs

ABSTRACT

This study investigated – for the first time – the simultaneous degradation of benzene, toluene, ethylbenzene and *o*-xylene (BTEX) by persulfate (PS) and peroxymonosulfate (PMS) activated by asphaltenes (Asph) under ultrasound (US) irradiation. Advantageous properties such as high thermal stability, low production cost and extensive availability make asphaltenes as an appealing carbonaceous material for heterogeneous catalysis. The application of asphaltenes in PS/US increased the degradation of BTEXs from 31%, 34%, 35%, 32%–78%, 94%, 98% and 98%, while the removal of these compounds in PMS/US system was improved from 26%, 27%, 24%, 20%–76%, 91%, 97%, 97%, respectively. PS and PMS activation followed a typical sulfate-radical based advanced oxidation processes. In terms of activation of PS and PMS, the particles of asphaltenes intensified formation of reactive radicals by creating additional centers of cavitational events. Moreover, owing to π–π stacking interaction between asphaltenes and sp^2-hybridized systems of BTEX, the contaminants undergo adsorption on the surface of asphaltenes and subsequent oxidation by formed radicals. The radical route of BTEX degradation in both PS/US/Asph and PMS/US/Asph systems was mainly contributed by sulfate ($SO_4^{\bullet -}$) and hydroxyl radicals ($HO^{\bullet}$) and coexisting superoxide radical anions ($O_2^{\bullet -}$) played a minor role.

1. Introduction

Hydrocarbons and volatile organic compounds (VOCs) play an important role among the substances determining the pollution of water and soil. According to European Union regulations, VOCs are defined as the organic compounds which possess initial boiling point

* Corresponding author.
E-mail address: grzegorz.boczkaj@pg.edu.pl (G. Boczkaj).

https://doi.org/10.1016/j.jhazmat.2020.122804
Received 11 March 2020; Received in revised form 25 April 2020; Accepted 25 April 2020
Available online 19 May 2020

below or equal to 250 °C at a standard atmospheric pressure of 101.3 kPa (EUR-Lex, 2020). Generally, most VOCs are toxic or odorous and regarded as the main contributor of photochemical smog, ozone depletion and global warming. Chemical, pharmaceutical, petrochemical, adhesives production and wastewater treatment plants are the main sources of VOCs. The petroleum hydrocarbon compounds are a group of organic constituents, which are components of gasoline and aviation fuels and are widely used in industrial syntheses. Crude oil, and in particular gasoline fraction is a main source of monoaromatic hydrocarbons, such as benzene, toluene, ethylbenzene and xylene isomers (BTEX) (Yadav and Reddy, 1993; Pawlowski Michael, 1998). These compounds are used as industrial solvents and they provide the starting materials for the production of many pharmaceuticals, agrochemicals, polymers, explosives, paints, cosmetics etc. (Smith, 1990). BTEX are frequently introduced into groundwater, soil and sediment by accidental spills and leakage from storage tanks and associated piping, improper waste disposal practice and leaching landfills as well as pollutants present in effluents discharged into the environment (Pawlowski Michael, 1998; Boczkaj and Fernandes, 2017; Liang et al., 2009). BTEX are known carcinogenic (Dean, 1985) and possess a negative impact on human being and the environment. Developing of efficient wastewater treatment technologies is compulsory to meet the standards of the stringent environment regulations.

In recent years, sulfate radical based advanced oxidation processes (S-AOPs) have been identified as alternative to classic AOPs and received a growing interest of researchers. S-AOPs generate and use sulfate radicals ($SO_4^{\bullet -}$), which possess a strong oxidation potential (2.6 V) (Chen and Su, 2012; Wang et al., 2015). As an oxidant, $SO_4^{\bullet -}$ radicals accept a single electron to yield SO_4^{2-} anions as follows (Liang and Bruell, 2008):

$$SO_4^{\bullet -} + e^- \rightarrow SO_4^{2-} \quad E^0 = 2.6\ V \tag{1}$$

$SO_4^{\bullet -}$ have longer half-life than $HO^{\bullet}$ (Oh et al., 2016). $SO_4^{\bullet -}$ prefer to react via electron-transfer mechanism, while $HO^{\bullet}$ react by addition, hydrogen-atom abstraction as well as electron-transfer mechanisms. As a result, $SO_4^{\bullet -}$ are selective in nature and prefer to react with electron donating groups such as hydroxyl ($-OH$), amino ($-NH_2$), alkoxy (–OR), π electrons of aromatic compounds, and unsaturated bonds. The reaction between $SO_4^{\bullet -}$ and electron withdrawing groups such as nitro ($-NO_2$) and carbonyl (C=O) groups is generally slower (Oh et al., 2016). Rastorgi and coworkers (Rastogi et al., 2009) concluded that the combination of high oxidation potential of $SO_4^{\bullet -}$ and slow consumption rate of precursor oxidants (stability) makes $SO_4^{\bullet -}$ very effective for the degradation of recalcitrant organic compounds. Two types of $SO_4^{\bullet -}$ precursors are commonly used in S-AOPs: (i) persulfate and (ii) peroxymonosulfate. Both persulfate anions ($S_2O_8^{2-}$) and peroxymonosulfate (HSO_5^-) can be activated by heat, UV-irradiation,-transition metal ions and heterogeneous catalysts to produce $SO_4^{\bullet -}$ (Wacławek et al., 2018, 2017). Among the activation approaches of PS and PMS, US irradiation with frequency of 20 − 40 kHz has received attention owing to the formation of cavities at the acoustic cavitation. This is the physical phenomenon which occurs when the passage of US through the cavitating medium generates cavities, promotes their growth and collapse. Cavitating bubbles generate localized high temperature and pressure in the reaction medium. Such conditions split water molecules leading to formation of highly reactive $HO^{\bullet}$, which are responsible for oxidation of organic contaminants. The removal efficiency of acoustic cavitation has been tested in degradation of various pollutants, including organic dyes, herbicides, organic sulfur compounds, alcohols, pharmaceuticals etc. Owing to the intensified formation of reactive species (radicals), the removal efficiency of acoustic cavitation was further improved by combination with AOPs. Hybrid processes based on acoustic cavitation coupled with various AOPs demonstrated high degradation rate of formic acid (Grčić et al., 2010), naphthol blue black dye (Reddy et al., 2016), 2-ethylthiophene, dibutyl sulfide, nitrobenzene, 2-nitrphenol, *m*-cresol, phenol (Gągol et al., 2018a, b) etc. A series of studies indicated that sono-activated PS is highly effective in removal of organic pollutants, such as bisphenol A (Darsinou et al., 2015), amoxicillin (Su et al., 2012), trichloroethane (Li et al., 2013), tetracycline (Hou et al., 2012), methyl *tert*-butyl ether (Neppolian et al., 2002), nitric oxide (Adewuyi and Owusu, 2006), 1,4-dioxane (Son et al., 2006), humic acid (Wang et al., 2015), dinitrotoluenes (Chen and Su, 2012) etc. In similar manner, sono-activated PMS was reported to be effective in degradation of sulfamethazine (Yin et al., 2018) and rhodamine B (Kurukutla et al., 2014).

The objective of the present study was to investigate the treatment of BTEX by PS and PMS activated by asphaltenes under US. The effect of PS and PMS concentration on BTEX degradation was examined. Free radical quenching studies were conducted to identify the active radical species involved in BTEX degradation. The stability of asphaltenes was examined by investigating the degradation of BTEX in PS/US and PMS/US systems at multiple catalytic cycles. To the best of our knowledge, there are no articles that reported the impact of asphaltenes on activation of PS and PMS toward oxidative removal of BTEX under US. Thus, the aim of this study is to investigate the effects of asphaltenes and oxidants on the US-assisted degradation of BTEX in the US/PS/Asph and US/PMS/Asph systems.

2. Materials and methods

2.1. Materials and chemicals

Sodium persulfate ($Na_2S_2O_8$), Oxone® (triple potassium salt, $2KHSO_5{\cdot}KHSO_4{\cdot}K_2SO_4$), toluene and methanol were purchased from POCH (Poland). Benzene, ethyl-benzene and *o*-xylene were purchased from Merck (Poland) and used as received. *p*-benzoquinone and *n*-heptane EMPLURA® (Merck, Germany) was used to isolate asphaltene fraction from bitumen 20/30 SDA (Lotos Group, Gdansk, Poland) and extract adsorbed BTEX from asphaltenes. *Tert*-butyl alcohol was purchased from Sigma-Aldrich (Germany). All chemicals and solvents were of analytical grade and were used without further purification.

2.2. Experimental procedures

BTEX degradation experiments were performed in ultrasonic bath (Sonorex RK 156 BH, Bandelin Electronic, Germany) operating at a fixed frequency of 35 kHz and a variable power output with a maximum of 860 W. Prior the experiment, aqueous solution of BTEX was solubilized by magnetic stirrer (1500 rpm) at room temperature (25 ± 2 °C) for 1 h. In a typical procedure, an amber colored glass containing 700 mL of aqueous solution of BTEX was placed at a certain position in ultrasonic bath. Solution of oxidant (PS or PMS) was added using HPLC pump, an outlet capillary of which was mounted in the bottom of the glass. Concentration of the oxidant varied depending on the ratio between generated radicals and BTEX (r_{ox}), while the flow rate of the oxidant injection was constant (1.4 mL/min). The reaction temperature of 25 ± 2 °C was maintained by refrigerated bath (Chrompack RTE-110B, Neslab Instruments, USA). Aliquots of samples with an approx. volume of 0.022 dm^3 were taken before the beginning of treatment, after every 15 min in the first hour of treatment and each hour until the end of the treatment. Radical scavenging agents were spiked into the reaction solution to distinguish $SO_4^{\bullet -}$, $HO^{\bullet}$ and $O_2^{\bullet -}$ radicals. To sufficiently quench the generated radicals, the molar ratio of 100:1 between scavenger and oxidant was used. All experiments were conducted in deionized water without any pH adjustment. pH was measured by Merck non-bleeding pH paper strips.

The isolation of asphaltenes was conducted according to the improved scalable method proposed and tested by (Plata-Gryl et al., 2018). Compared to standard separation techniques, the novel method ensures the isolation of asphaltene fraction with superior purity and improved reproducibility. The method consists of filtration through a

cellulosic thimble and extensive washing in a Soxhlet type reactor. To evaluate the risk of asphaltenes leaching into solution, including releasing of polycyclic aromatic hydrocarbons (PAHs), a UV spectra of liquid processed by sonocavitation with sole PS or PMS were compared with processes performed with presence of asphaltenes. The solutions were filtrated by 045 μm PTFE filters and the spectra were measured in 300 − 800 nm range (characteristic for polycyclic aromatics) using a DR5000 (HACH Lange) UV spectrophotometer.

2.3. Methods

The degradation of BTEX was monitored by an auto system gas chromatograph with a flame ionization detector (GC-FID) (Perkin Elmer, Clarus 500, USA). Quantitative analysis was carried out using the internal standard method (4-chlorophenol). Retention time of benzene, toluene, ethylbenzene, *o*-xylene and the internal standard was 11.10 min, 14.64 min, 17.36 min, 18.04 min and 18.93 min, respectively (Supplementary Figure S1). 10 μL of aqueous solution of 4-chlorophenol (10 mg/mL) was injected to 10 mL of each sample during the sample preparation, which was done by dispersive liquid-liquid microextraction (DLLME). The mixture of 0.4 mL acetone and 0.5 mL dichloromethane was added with a subsequent shaking for 1 min and centrifugation at 4000 rpm for 8 min (EBA 8S, Hettich, Germany). A volume of 250 μL of the sedimented organic phase was then transferred to 2 mL vials equipped with 300 μL micro inserts. The vials were placed in an autosampler. Finally, 2 μL of the extract was analyzed by GC-FID. The procedure of BTEX analysis was described elsewhere in a dedicated paper (Makoś et al., 2018). Briefly, the procedure provide a very good analytical performance (in terms of sensitivity, linearity and reproducibility) and was developed especially for the needs of process control during AOPs studies. The limit of detection values (LOD) for BTEXs are 1.8, 2.3, 1.5, 3.6 μg/L. The limits of quantitation (LOQ) are equal to 3*LOD.

3. Results and discussion

3.1. Activation of PS and PMS under sonocavitation conditions

The use of US as an AOP relies on its ability of $HO^{\bullet}$ formation in aqueous solution and subsequent degradation of contaminants by $HO^{\bullet}$. $HO^{\bullet}$ are formed due to decomposition of water molecules caused by acoustic cavitation (sonocavitation), which takes place in a liquid as a result of vibrations induced by US. US initiates the growth and subsequent collapse of cavitational bubbles, which is accompanied with a release of a large magnitude of temperature and pressure. During this process, pyrolytic decomposition of water occurs inside the bubble as well as in interfacial region between the gaseous phase and surrounding liquid. Furthermore, application of US generates local turbulence and acoustic streaming, thus decreasing the limits related to mass transfer in the reaction mixture.

Similar to conventional activation methods, the energy emitted during the collapse of the cavitation bubble could accelerate PS and PMS to produce $SO_4^{\bullet -}$ (Price and Clifton, 1996; Ghanbari and Moradi, 2017). Sono-activated PS and PMS have received a great attention as a potential alternative for the degradation of recalcitrant organic contaminants in wastewater treatment. Both processes were found to consist of many reverse and side reactions resulting in formation of $SO_4^{\bullet -}$, $HO^{\bullet}$ and $SO_5^{\bullet -}$ (Ghanbari and Moradi, 2017; Wang and Zhou, 2016).

The US irradiation can induce a cavitation phenomenon, which is a crucial factor in the systems involving sono-activation of PS and PMS. Therefore, sonolytic experiments were carried out to evaluate and verify the effectiveness of US assisted PS and PMS processes. The degradation of BTEX in sole US, PS, PMS processes was evaluated and displayed in Fig. 1 and 2. It can be seen that a negligible degradation degree was obtained when sonication alone was used to treat BTEX as a very small amount of $HO^{\bullet}$ was formed. In addition, no large increase of BTEX decomposition appeared during sole PS and PMS processes due to the limited oxidation capacity of the oxidants and stability at ambient conditions.

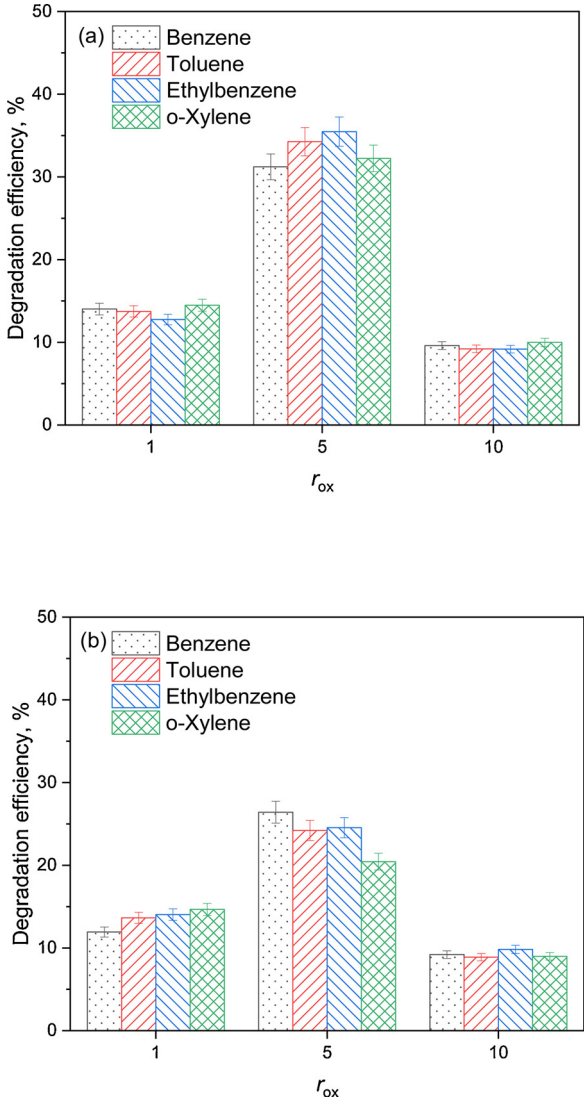

Fig. 1. Effects of PS (a) and PMS (b) concentration on BTEX degradation under US. Experimental conditions: $[BTEX]_0$ = 40 mg/L, T = 25 ± 2 °C, $[pH]_0$ = 5.0, t = 360 min. Molar ratio of the oxidant to BTEX (r_{ox}): r_{ox}1 [PS/PMS]:[BTEX] = 1:1, r_{ox}5 [PS/PMS]:[BTEX] = 5:1, r_{ox}10 [PS/PMS]:[BTEX] = 10:1.

When the PS was combined with US, the degradation degree of benzene, toluene, ethylbenzene, *o*-xylene was 14.0%, 13.7%, 12.7% and 14.5%, respectively. As well as US/PS, PMS coupled with US showed higher removal of BTEX than the sum of the removal efficiencies when BTEX was individually treated by sole US and PMS processes. These results indicate the intensification of radical production due to activation of PS and PMS by US irradiation.

It is commonly assumed that in various activated PS and PMS systems, the increase of the relative amount of the precursor oxidant would result in subsequent elevated generation of $SO_4^{\bullet -}$, and thus could enhance the degradation rate of contaminants. However, above some limiting concentration level, the degradation decreases. It follows from the scavenging effect of PS or PMS in the solution in relation to produced $SO_4^{\bullet -}$ and $HO^{\bullet}$. This behavior was confirmed in several papers thus determination of an optimal oxidant concentration is necessary for effective application of S-AOPs in wastewater treatment. To evaluate the possible use of PS and PMS for the treatment of volatile

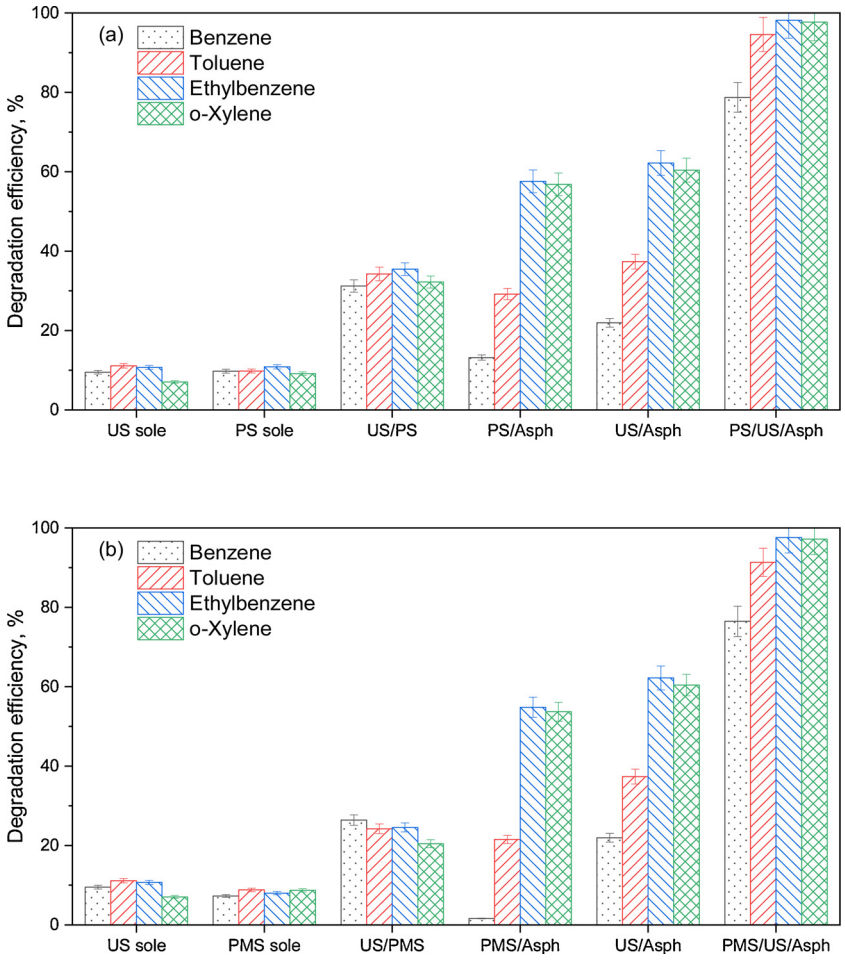

Fig. 2. Effect of asphaltenes on BTEX degradation over sono-activated PS and PMS. Experimental conditions: $[BTEX]_0$ = 40 mg/L, T = 25 ± 2 °C, $[pH]_0$ = 5.0, $[Asph]_0$ = 0.5 g/L, t =360 min, [PS/PMS]:[BTEX] = 5:1 (r_{ox} = 5).

aromatics, the effect of initial PS and PMS concentrations was studied at three molar ratios of oxidant to BTEX (r_{ox} 1, 5 and 10).

Fig. 2 illustrates the influence of PS and PMS concentration on the oxidative degradation of BTEX in aqueous solution under ambient conditions. It can be seen that the degradation efficiency of BTEX exhibits an increasing tendency with the increase of the BTEX to oxidant ratio in both sono-activated PS and PMS systems. Besides, in case of PS process (Fig. 1a) with r_{ox} 5, the removal percentage of BTEX was obviously higher than those of r_{ox} 1 and 10. For instance, the degradation of benzene after the treatment time of 360 min exceeded 31% at r_{ox} 5, while 14.0 and 10% of benzene was removed at r_{ox} 1 and 10, respectively, during the same time period. Similar BTEX degradation efficiency with a slightly lower extend was observed for PMS processes with r_{ox} 1, 5, 10. Thus, 26% of benzene was degraded at r_{ox} 5, while the degradation efficiency of benzene reached 11% and 9% at r_{ox} 1 and 10, respectively. It has been reported that the accelerated formation of sulfate radicals is the main factor contributing to the oxidative degradation of contaminants in sono-activated PS and PMS systems. Therefore, higher level of $SO_4^{\bullet-}$ is produced at r_{ox} 5 compared to r_{ox} 1 which led to higher degradation of BTEX at r_{ox} 5. On the other hand, adoption of higher initial dosage of PS (r_{ox} 10) led to the lower degradation efficiency, which can be attributed to the competitive consumption of $SO_4^{\bullet-}$ with residual (unreacted) PS yielding less effective $S_2O_8^{\bullet-}$ (Ferkous et al., 2017):

$$SO_4^{\bullet-} + S_2O_8^{2-} \rightarrow SO_4^{2-} + S_2O_8^{\bullet-} \quad (2)$$

3.2. Effect of asphaltenes

Activation of PS and PMS to generate $SO_4^{\bullet-}$ is also possible by using carbon-based materials as catalysts. These materials include modifications of carbon, such as activated carbon, graphene oxide, nanodiamond, carbon nanotubes and graphite (Ghanbari and Moradi, 2017; Ouyang et al., 2017). Up to date, iron activated carbon (Ma et al., 2017), granular activated carbon loaded with Fe (II) (Li et al., 2016), biochar-supported nano magnetite (Ouyang et al., 2017) have been reported to efficiently activate PS, while successful activation of PMS was demonstrated using reduced graphene oxide (Sun et al., 2012), graphitic carbon nitride (Feng et al., 2018; Li et al., 2018), N-doped graphene (Liang et al., 2017). In most cases these compounds were reported to activate PS/PMS by donating electrons from functional groups (C═O) and sp^2-hybridized lattice. Although the appealing results, the mechanism of PS and PMS activation assisted by carbonaceous catalysts is still under discussion. An interesting group of compounds that could be an alternative to currently studied materials are asphaltenes. Asphaltenes are polycyclic aromatic compounds with a molecular structure composed of highly fused aromatic rings, peripherally attached alkyl chains and polar functional groups, e.g., carboxylic acids, phenol and pyridines. Besides hydrogen and carbon, the chemical composition of asphaltenes contains heteroatoms such as oxygen, sulfur, nitrogen, trace amounts of vanadium and nickel, which can be found in their backbone (Plata-Gryl et al., 2018; Groenzin and Mullins, 2000). In similar manner with multiwalled carbon nanotubes, the sp^2 covalent carbon network along with oxygen-containing functional groups of asphaltenes may conduct a redox cycle for electron

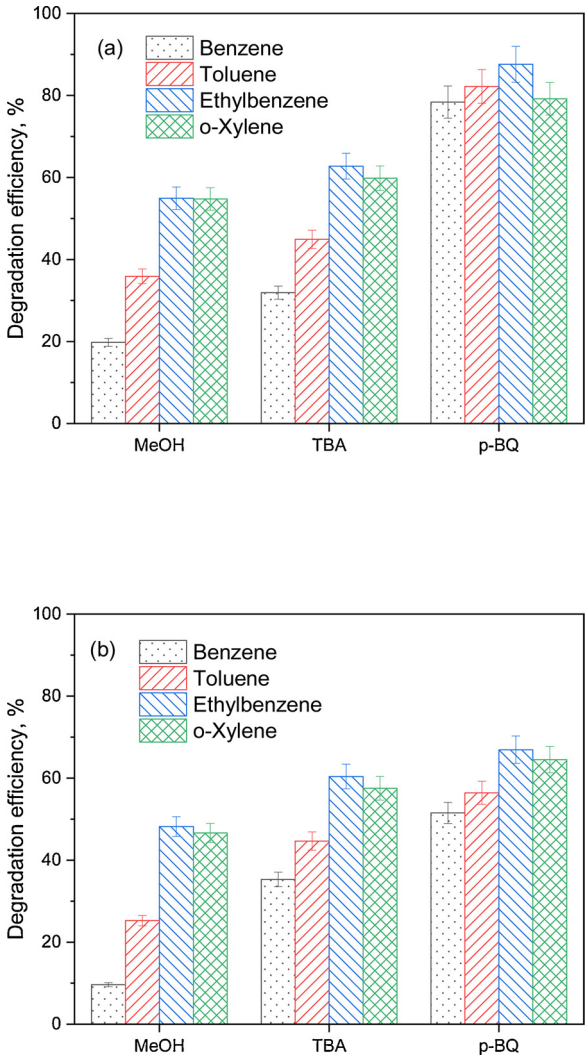

Fig. 3. Effect of radical scavengers on BTEX degradation over sono-activated PS (a) and PMS (b) in presence of asphaltenes. Experimental conditions: $[BTEX]_0$ = 40 mg/L, [MeOH] = 30 g/L, [TBA] = 69 g/L, [*p*-BQ] = 101 g/L, T = 25 ± 2 °C, $[pH]_0$ = 5.0, $[Asph]_0$ = 0.5 g/L, t = 360 min, [PS/PMS]:[BTEX] = 5:1 (r_{ox} = 5).

transfer to PS or PMS to produce radicals just like the activation of these oxidants by transition metals (Duan et al., 2015).

In order to comprehensively evaluate the catalytic activity of asphaltenes on BTEX degradation in PS/US/Asph and PMS/US/Asph systems, a series of comparative experiments were conducted using a catalyst dosage of 0.5 g/L and oxidants dosage of r_{ox} 5. As shown in Fig. 2a, US alone degraded a negligible amount (9.5%, 11.1%, 10.7%, 7.1% of benzene, ethylbenzene, toluene and *o*-xylene, respectively) of BTEX after 360 min of treatment. The degradation efficiency of each BTEX component was then improved after adding PS and PMS. Thus, in the sole PS/US system, the degradation of benzene reached 31.2%, whereas 34.3%, 35.5%, 32.2% of toluene, ethylbenzene and *o*-xylene, respectively, in 360 min. Although PMS was reported to be easily activated and produce sulfate radicals compared to PS, PMS/US system exhibited slightly lower efficiency than PS/US system degrading 26.4%, 24.2%, 24.5%, 20.4% of benzene, toluene, ethylbenzene and *o*-xylene, respectively.

Degradation efficiencies were considerably increased for both PS/US and PMS/US systems in presence of asphaltenes indicating their potential use in catalytically degradation of BTEX. To investigate the contribution of BTEX adsorption on asphaltenes, after the degradation test, asphaltenes were filtered and treated with n-pentane to extract residual BTEX from the catalyst. This protocol was validated by a series of experiments for different solvents, which revealed, that n-pentane is able to almost quantitatively (> 99%) desorb BTEXs from the asphaltene surface.

The study revealed, that asphaltenes are an effective adsorbent for BTEX removal from water. A primary model solution of BTEX containing 0.5 g/L of asphaltenes was prepared and stirred for 60 min to reach the adsorption-desorption equilibrium. After reaching equilibrium, the content of benzene, toluene, ethylbenzene and *o*-xylene in water were decreased by 9%, 29%, 53%, 53%, respectively, indicating high adsorption capacity of asphaltenes. Addition of PS or PMS at optimal conditions resulted in further increase of BTEX removal. However, total removal of BTEX can be caused by adsorption or mixed mode of oxidation with adsorption. A GC-FID analysis of the extracted phase (by *n*-pentane) from asphaltenes after PS/US/Asph and PMS/US/Asph processes revealed a lack of residual benzene and toluene remaining on asphaltene surface and a minimal concentration of remaining ethylbenzene and *o*-xylene. Asphaltenes separated after PS/US/Asph process contain a less than 1% of both ethylbenzene and *o*-xylene primary amount. On the other hand, the analysis of *n*-pentane, which was used to extract BTEX from asphaltenes used in PMS/US/Asph process revealed the presence of 3% and 2% of ethylbenzene and *o*-xylene, respectively. Based on these results, it is clear that in both cases the removal of BTEX via cavitation was intensified in the presence of asphaltenes. The sono-catalytic process resulted in 78%, 94%, 98%, 98% removal of benzene, toluene, ethylbenzene and *o*-xylene in case of PS application, respectively. These compounds have been correspondingly degraded by 76%, 91%, 97%, 97% in PMS/US/Asph process as depicted in Fig. 2b. Particularly, the synergistic index of PS/US/Asph and PMS/US/Asph processes in the degradation of ethylbenzene were determined as 4.07 and 4.12 applying Eq. (3), respectively.

$$\text{Synergistic index (PS or PS/US/Asph)} = \frac{k\,(\text{PS or PS/US/Asph})}{k\,(\text{US}) + k\,(\text{PS or PMS/Asph})} \quad (3)$$

Where k denotes the apparent rate constant (k_{app}) of the combined and the individual processes. The degradation rate of BTEX fitted the pseudo-first-order reaction kinetic model and the corresponding k_{app} was determined from $\ln(C/C_0) = -k_{app}t$, where C and C_0 represent the concentration of BTEX components at the time t and 0 min, respectively.

The synergistic catalytic effect of the hybrid process in the degradation of BTEX in aqueous solution can be ascribed to the crucial contribution of asphaltenes in terms of activation of PS/PMS under US irradiation. Thus, solid particles of asphaltenes dispersed in the solution adsorb BTEX and creates additional centers of cavitational events, which induce the activation of PS and PMS. In this condition, BTEX primarily adsorbed on the surface of asphaltenes undergo pyrolytic decomposition inside the cavitation bubble, where the factor of mass transfer limited by the diffusion of BTEX from the bulk liquid to interfacial region is neglected. Activation of radical precursors (PS, PMS) takes place in the interfacial region and the produced radicals can rapidly react with contaminant molecules. $HO^{\bullet}$ can also be produced by the depletion of water molecules in the interfacial region. The contribution of $HO^{\bullet}$ during cavitation in presence of asphaltenes is depicted in Fig.2a as US/Asph process. As it can be seen from Fig.3, 21%, 37%, 62%, 60% of benzene, toluene, ethylbenzene and *o*-xylene, respectively, were degraded by US/Asph process, which is higher than the removal efficiency of US/PS and US/PMS processes. This can be ascribed to the greater amount of cavitation bubbles generated on the immersed asphaltenes. On the other hand, activation of PS and PMS as well as the oxidation of BTEX can be mediated by electron transfer, in which the surface of asphaltenes plays a critical role, bringing together electron donor and acceptor pairs to a close proximity (Lee et al., 2016). In such scenario, BTEX molecules adsorbed on the surface of

asphaltenes donate a single electron to PS and PMS along the carbon network of asphaltenes facilitated by oxygen-containing functional groups.

3.3. Determination of radicals present in PS/US/Asph and PMS/US/Asph systems

The oxidation mechanism of S-AOPs is complex and involves generation, consumption and recombination of $SO_4^{\bullet -}$ and $HO^{\bullet}$, responsible species for the destruction of organic contaminants. To elucidate the reaction mechanism and evaluate the contribution of these reactive species towards BTEX degradation, radical scavenger experiments were conducted using selective radical quenching agents, such as methanol (MeOH), *tert*-butyl alcohol (TBA) and *p*-benzoquinone (*p*-BQ). According to literature, the scavenging rate constant of MeOH is $9.7 \times 10^8\ M^{-1}\ s^{-1}$ for $HO^{\bullet}$ and $3.2 \times 10^6\ M^{-1}\ s^{-1}$ for $SO_4^{\bullet -}$. Thus, MeOH, containing α-hydrogen, can rapidly quench both $HO^{\bullet}$ and $SO_4^{\bullet -}$. In contrast, TBA selectively quench $HO^{\bullet}$, as its rate constant with $HO^{\bullet}$ ($6.0 \times 10^8\ M^{-1}\ s^{-1}$) is much greater than that with $SO_4^{\bullet -}$ ($4.0 \times 10^5\ M^{-1}\ s^{-1}$). In addition, *p*-BQ was used to capture superoxide anion radicals ($O_2^{\bullet -}$) as they react rapidly with a rate constant of $0.9-1 \times 10^9\ M^{-1}\ s^{-1}$ (Fan et al., 2019). Monitoring the degradation efficiency of BTEX upon addition of these scavengers would provide an insight on predominant radical species responsible for the oxidative degradation of BTEX.

Fig. 3a presents the effects of MeOH, TBA and *p*-BQ on BTEX degradation by sono-activated PS under ambient conditions. MeOH significantly suppressed the degradation efficiency of benzene, toluene, ethylbenzene, *o*-xylene from 78.7%, 94%, 98.2%, 97.7%–19.8%, 35.9%, 54.9%, 54.7%, respectively, demonstrating that both $SO_4^{\bullet -}$ and $HO^{\bullet}$ are generated and contributed to the BTEX degradation during PS/US/Asph process. Removal efficiency of benzene, toluene, ethylbenzene and o-xylene obtained in the presence of TBA reached 31.9%, 44.9%, 62.7% and 59.8%, respectively, and was slightly higher than those of MeOH. This indicates that $SO_4^{\bullet -}$ are the dominant reactive radical species involved in BTEX degradation by PS/US/Asph system. Furthermore, when *p*-BQ was added to the reaction mixture, the removal efficiency of BTEX was only slightly inhibited suggesting that small amount of $O_2^{\bullet -}$ is generated in PS/US/Asph system. For instance, the degradation efficiency of toluene was 82.2%, which shows that the removal of toluene was suppressed by only 11.8%. These results clearly indicate that the relative contribution of reactive species towards BTEX degradation by PS/US/Asph process follow the order: $SO_4^{\bullet -} > HO^{\bullet} > O_2^{\bullet -}$.

Second series of radical scavenging experiments were performed for PMS/US/Asph process. As shown in Fig. 3b, significant reduction in the degradation of BTEX occurs in presence of either MeOH or TBA. Addition of MeOH markedly inhibited the degradation of benzene, toluene, ethylbenzene and *o*-xylene from 76%, 91%, 97%, 97% to 9%, 25%, 48% 46%, respectively, in 360 min treatment. Moreover, TBA decreased the removal efficiency of benzene, toluene, ethylbenzene and *o*-xylene to 35.3%, 44.6%, 60.4% and 57.5%, respectively. These results indicated, that MeOH had much more inhibitory effect than TBA on the degradation efficiency of BTEX. Therefore, it can be suggested that both $SO_4^{\bullet -}$ and $HO^{\bullet}$ are formed in PMS/US/Asph system and contribute to the BETX degradation. However, $SO_4^{\bullet -}$ appeared to be the main oxidizing species in PMS/US/Asph system. Further tests with the addition of *p*-BQ led to slight decrease of BTEX degradation efficiency, suggesting the formation and coexisting of $O_2^{\bullet -}$. It has been reported that $O_2^{\bullet -}$ were produced during PMS activation by Mn-doped g-C_3N_4 composites and mediated the catalytic degradation of acetaminophen (Fan et al., 2019). The formation of $O_2^{\bullet -}$ was concluded to take place on the surface of the composites due to the reaction of Mn(II) and Mn (III) deposited in the N-pot with HSO_5^-. Similarly, $O_2^{\bullet -}$ along with $^1O_2$ were identified as the dominant reactive species involved in Pd/g-C_3N_4-PMS system (Wang et al., 2017). In case of PMS/US/Asph system, the formation of radicals occurs mainly in the interfacial zone of the imploding bubble and the formation of $O_2^{\bullet -}$ via electron donating mechanism from trace transition metals is negligible. Metal-doped carbonaceous materials are known to produce $O_2^{\bullet -}$ due to the reaction of dissolved O_2 with transition metals. $O_2^{\bullet -}$ possess an affinity to the surface of metal oxide, where it reacts with contaminant molecules leading to their destruction. Interaction of dissolved O_2 with the trace amount of transition metals in PMS/US/Asph system is suppressed due to hydrophobic properties of asphaltenes. Thus, it can be suggested that $O_2^{\bullet -}$ in the PMS/US/Asph system are produced by self-decomposition of PMS as previously reported by Li et al. (Eqs. (4) and (5)) (Li et al., 2020):

$$HSO_5^- \rightarrow SO_5^{2-} + H^+ \quad (4)$$

$$SO_5^{2-} + H_2O \rightarrow O_2^{\bullet -} + SO_4^{2-} + 2H^+ \quad (5)$$

3.4. Reusability and stability of asphaltenes in PS/US and PMS/US systems

Application of metal-based catalysts in industrial sectors require good reusability and minimal secondary contamination caused by leaching of noxious transition metal ions. Stability of the catalyst during heterogeneous oxidation of contaminants is a crucial factor determining the recyclability. Herein, to investigate the reusability of asphaltenes, three recycling experiments of BTEX degradation over both Asph/PS/US and Asph/PMS/US systems were performed. In a standard experimental procedure, the catalyst was isolated via vacuum filtration after each cycle and was then collected for use in the next cycle. The catalyst was isolated using hydrophilic PTFE membrane filters with pore size of 0.45 μm and washed with deionized water.

Fig. 4a illustrates the reusability of asphaltenes in BTEX degradation by PS/US. It can be seen that the degradation efficiency of benzene, toluene, ethylbenzene and *o*-xylene at 360 min at second cycle reached 42.3%, 55.8%, 65.6% and 62.4%, respectively. This indicates a decrease of catalytic properties by approx. 30%. Similar effect was observed for Asph/PMS/US system (Fig. 4b). Further repetitive experiments for third cycle consequently decreased the degradation efficiency of asphaltenes in both asphaltenes-based catalytic systems, i.e., Asph/PS/US and Asph/PMS/US. Such reduction of the catalytic activity is comparable to supported metal-based catalyst used to activate PS and PMS (Shukla et al., 2011).

It has been well reported that the deactivation of metal-based catalysts is commonly attributed to the changes of surface crystal structure and surface coverage by reaction intermediates (Sun et al., 2012; Rong et al., 2019). In case of asphaltenes, aromatic hydrocarbons and intermediates quickly cover the catalyst surface due to their strong interaction with sp^2 hybridized system (Groenzin and Mullins, 2000). Comparison of the third sequential runs reveals greater decrease of asphaltenes catalytic properties in activation of PS than PMS. This can be attributed to the reduction of active sites due to the consumption of metal activators by PS as described in Eq. (5). In contrast, charge of the metal activator during PMS activation is recovered with formation of $SO_5^{\bullet -}$ (Eqs. (6) and (7)) (Oh et al., 2015):

$$S_2O_8^{2-} + Me^{n+} \rightarrow Me^{(n+1)+} + SO_4^{2-} + SO_4^{\bullet -} \quad (6)$$

$$HSO_5^- + Me^{n+} \rightarrow Me^{(n+1)+} + HO^- + SO_4^{\bullet -} \quad (7)$$

$$HSO_5^- + Me^{(n+1)+} \rightarrow Me^{n+} + H^+ + SO_5^{\bullet -} \quad (8)$$

However, different disposal scenarios of the catalysts after treatment process can be proposed for asphaltenes – in contrast to other type of catalysts used for S-AOPs. Asphaltenes are components of bitumen. Their presence along with resins fraction is desired for road bitumen applications. They are intentionally formed during a so-called bitumen blowing process, where hot air is introduced to residuum of vacuum distillation of crude oil. Secondly an asphaltenes-rich stream is obtained as a raffinate fraction from Residual Oil Solvent Extraction (ROSE)

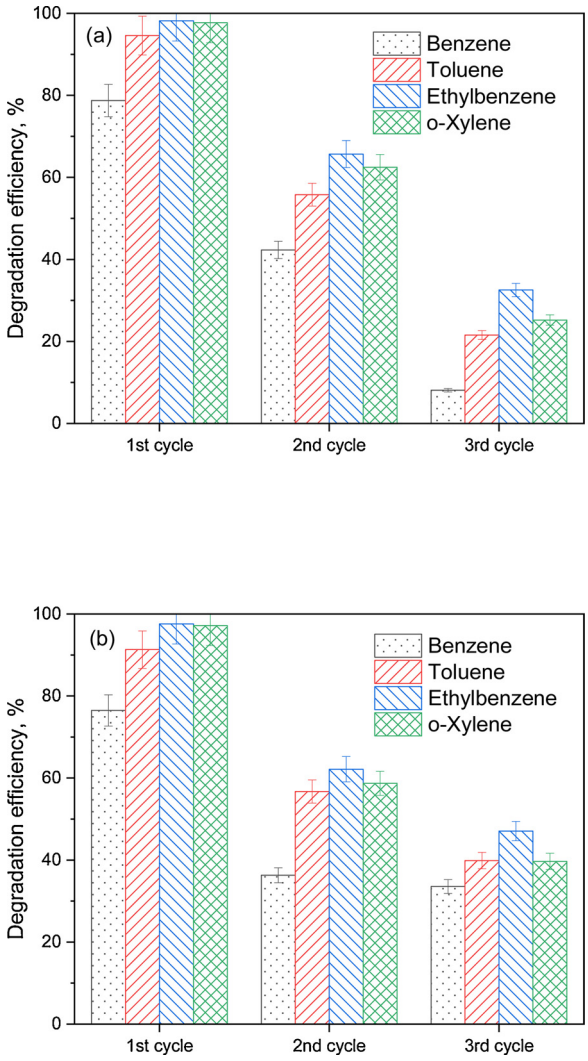

Fig. 4. Reusability of asphaltenes in Asph/PS/US (a) and Asph/PMS/US (b) systems for the degradation of BTEX. Experimental conditions: $[BTEX]_0$ = 40 mg/L, T = 25 ± 2 °C, $[pH]_0$ = 5.0, $[Asph]_0$ = 0.5 g/L, t = 360 min, [PS/PMS]:[BTEX] = 5:1 (r_{ox} = 5).

process. Their industrial scale production is less expensive and robust – based on precipitation of asphaltenes by alkanes from residuum of vacuum distillation of crude oil or oxidized bitumen. Thus, their recycling is not obligatory and even one-batch applications at proved effectiveness can be described as satisfactory. Also, their disposal is obvious – they can be added to different type of bitumen to produce a blended bitumen having desired asphaltenes content. In case of addition of wasted asphaltenes to the feedstock used for bitumen blowing, even presence of water is acceptable. Water is injected during oxidation to control the temperature (its evaporation during exothermal bitumen oxidation allows to cool the oxidized bitumen and prevent its local overheating). This way, the application of asphaltenes as a catalyst for S-AOPs would be based on a closed-cycle, which in overall is not affecting the life cycle assessment of this material.

The asphaltenes used in this study are expected to be free of any components that could be leached into the solution. It is assured by preparation procedure (Plata-Gryl et al., 2018), which include a Soxhlet extraction stage with n-heptane. During the studies described in (Plata-Gryl et al., 2018) a series of experiments was performed using also different solvents for Soxhlet extraction. It included application of methanol (MeOH) as well as water for second stage extraction after n-heptane. In both cases, analysis of post-extraction solutions of MeOH or water revealed a lack of increase of absorbance measured for UV and Vis range of the spectrophotometer.

However, theoretically some polycyclic aromatic hydrocarbons could be introduced into the treated solution during applications of ultrasounds and strong oxidants. To detect the possible leaching of polycyclic aromatic hydrocarbons (PAHs), asphaltenes were placed in blank solution of deionized water containing PS or PMS equal to r_{ox} 5 process and sonicated for 360 min. Then the post-process liquid was filtered and analyzed by UV–vis spectrophotometer to identify the presence of leached asphaltenes. A 300 – 800 nm range was selected on the basis of PAHs spectra. As seen in Fig. S2, the overlay of acquired UV spectra clearly shows, that there is no change in the absorbance for studied range comparing sole use of oxidants with the catalytic – asphaltene-aided systems.

It confirms that no leaching of PAH related compounds occurred during the treatment process.

4. Conclusions

The present study demonstrates the first attempt on using asphaltenes for activation of PS and PMS under US irradiation. Although, PS and PMS can be activated under US, PS-US and PMS-US processes were found insufficient to remove BTEX. Asphaltenes assisted by US exhibited high heterogeneous catalytic activity towards both PS and PMS activation, resulting in efficient simultaneous BTEX degradation. At the optimal conditions - catalyst loading of 0.5 g/L and r_{ox} 5, PS/US/Asph degraded 78%, 94%, 98% and 97% of benzene, toluene, ethylbenzene and *o*-xylene, respectively, while 76%, 91%, 97%, 97% of those compounds were correspondingly degraded by PMS/US/Asph. High adsorption capacity of asphaltenes combined with acoustic cavitation induced by US resulted in a synergistic effect in activation of PS and PMS and BTEX removal. $SO_4^{\bullet -}$ and $HO^{\bullet}$ were found to be the major active chemical species generated during PS and PMS activation in PS/US/Asph and PMS/US/Asph systems. A minor role of $O_2^{\bullet -}$ in BTEX degradation was also confirmed in PMS/US/Asph system, verified *p*-BQ scavenging test.

CRediT authorship contribution statement

Kirill Fedorov: Investigation, Formal analysis, Writing - original draft, Conceptualization, Methodology, Validation, Data curation. **Maksymilian Plata-Gryl:** Investigation, Methodology, Validation, Formal analysis, Writing - original draft, Conceptualization. **Javed Ali Khan:** Validation, Writing - review & editing. **Grzegorz Boczkaj:** Conceptualization, Methodology, Validation, Investigation, Formal analysis, Writing - original draft, Writing - review & editing, Supervision, Project administration, Funding acquisition.

Declaration of Competing Interest

The authors declare that they have no known competing financial interests or personal relationships that could have appeared to influence the work reported in this paper.

Acknowledgements

The authors gratefully acknowledge financial support from the National Science Centre, Warsaw, Poland for project OPUS nr UMO-2017/25/B/ST8/01364 and from the National Center for Research and Development, Warsaw, Poland – Project LIDER, no. LIDER/036/573/L-5/13/NCBR/2014. The authors are thankful for the Lotos Asfalt, Ltd. (Grupa Lotos) for their cooperation on this project. The authors have declared no competing financial interest.

Appendix A. Supplementary data

Supplementary material related to this article can be found, in the online version, at doi:https://doi.org/10.1016/j.jhazmat.2020.122804.

References

Adewuyi, Y.G., Owusu, S.O., 2006. Ultrasound-induced aqueous removal of nitric oxide from flue gases: effects of sulfur dioxide, chloride, and chemical oxidant. J. Phys. Chem. A 110, 11098–11107. https://doi.org/10.1021/jp0631634.

Boczkaj, G., Fernandes, A., 2017. Wastewater treatment by means of advanced oxidation processes at basic pH conditions: a review. Chem. Eng. J. 320, 608–633. https://doi.org/10.1016/J.CEJ.2017.03.084.

Chen, W.-S., Su, Y.-C., 2012. Removal of dinitrotoluenes in wastewater by sono-activated persulfate. Ultrason. Sonochem. 19, 921–927. https://doi.org/10.1016/J.ULTSONCH.2011.12.012.

Darsinou, B., Frontistis, Z., Antonopoulou, M., Konstantinou, I., Mantzavinos, D., 2015. Sono-activated persulfate oxidation of bisphenol A: Kinetics, pathways and the controversial role of temperature. Chem. Eng. J. 280, 623–633. https://doi.org/10.1016/J.CEJ.2015.06.061.

Dean, B.J., 1985. Recent findings on the genetic toxicology of benzene, toluene, xylenes and phenols. Mutat. Res. Genet. Toxicol. Environ. Mutagen. 154, 153–181. https://doi.org/10.1016/0165-1110(85)90016-8.

Duan, X., Sun, H., Kang, J., Wang, Y., Indrawirawan, S., Wang, S., 2015. Insights into heterogeneous catalysis of persulfate activation on dimensional-structured nanocarbons. ACS Catal. 5, 4629–4636. https://doi.org/10.1021/acscatal.5b00774.

EUR-Lex, EUR-Lex - 32004L0042 - EN, 2004.

Fan, J., Qin, H., Jiang, S., 2019. Mn-doped g-C3N4 composite to activate peroxymonosulfate for acetaminophen degradation: the role of superoxide anion and singlet oxygen. Chem. Eng. J. 359, 723–732. https://doi.org/10.1016/J.CEJ.2018.11.165.

Feng, Y., Liao, C., Kong, L., Wu, D., Liu, Y., Lee, P.H., Shih, K., 2018. Facile synthesis of highly reactive and stable Fe-doped g-C3N4 composites for peroxymonosulfate activation: a novel nonradical oxidation process. J. Hazard. Mater. https://doi.org/10.1016/j.jhazmat.2018.04.056.

Ferkous, H., Merouani, S., Hamdaoui, O., Pétrier, C., 2017. Persulfate-enhanced sonochemical degradation of naphthol blue black in water: evidence of sulfate radical formation. Ultrason. Sonochem. 34, 580–587. https://doi.org/10.1016/J.ULTSONCH.2016.06.027.

Gągol, M., Przyjazny, A., Boczkaj, G., 2018a. Highly effective degradation of selected groups of organic compounds by cavitation based AOPs under basic pH conditions. Ultrason. Sonochem. 45, 257–266. https://doi.org/10.1016/J.ULTSONCH.2018.03.013.

Gągol, M., Przyjazny, A., Boczkaj, G., 2018b. Wastewater treatment by means of advanced oxidation processes based on cavitation – a review. Chem. Eng. J. 338, 599–627. https://doi.org/10.1016/J.CEJ.2018.01.049.

Ghanbari, F., Moradi, M., 2017. Application of peroxymonosulfate and its activation methods for degradation of environmental organic pollutants: review. Chem. Eng. J. 310, 41–62. https://doi.org/10.1016/J.CEJ.2016.10.064.

Grčić, I., Obradović, M., Vujević, D., Koprivanac, N., 2010. Sono-Fenton oxidation of formic acid/formate ions in an aqueous solution: from an experimental design to the mechanistic modeling. Chem. Eng. J. 164, 196–207. https://doi.org/10.1016/J.CEJ.2010.08.059.

Groenzin, H., Mullins, O.C., 2000. Molecular size and structure of asphaltenes from various sources. Energy Fuels 14, 677–684. https://doi.org/10.1021/ef990225z.

Hou, L., Zhang, H., Xue, X., 2012. Ultrasound enhanced heterogeneous activation of peroxydisulfate by magnetite catalyst for the degradation of tetracycline in water. Sep. Purif. Technol. 84, 147–152. https://doi.org/10.1016/J.SEPPUR.2011.06.023.

Kurukutla, A.B., Kumar, P.S.S., Anandan, S., Sivasankar, T., 2014. Sonochemical degradation of rhodamine B using oxidants, hydrogen Peroxide/Peroxydisulfate/Peroxymonosulfate, with Fe2+ ion: proposed pathway and kinetics. Environ. Eng. Sci. 32, 129–140. https://doi.org/10.1089/ees.2014.0328.

Lee, H., Kim, H., Weon, S., Choi, W., Hwang, Y.S., Seo, J., Lee, C., Kim, J.-H., 2016. Activation of Persulfates by Graphitized Nanodiamonds for removal of organic compounds. Environ. Sci. Technol. 50, 10134–10142. https://doi.org/10.1021/acs.est.6b02079.

Li, B., Li, L., Lin, K., Zhang, W., Lu, S., Luo, Q., 2013. Removal of 1,1,1-trichloroethane from aqueous solution by a sono-activated persulfate process. Ultrason. Sonochem. 20, 855–863. https://doi.org/10.1016/J.ULTSONCH.2012.11.014.

Li, Z., Yang, Q., Zhong, Y., Li, X., Zhou, L., Li, X., Zeng, G., 2016. Granular activated carbon supported iron as a heterogeneous persulfate catalyst for the pretreatment of mature landfill leachate. RSC Adv. https://doi.org/10.1039/c5ra21781d.

Li, H., Shan, C., Pan, B., 2018. Fe(III)-Doped g-C3N4 mediated peroxymonosulfate activation for selective degradation of phenolic compounds via high-valent iron-oxo species. Environ. Sci. Technol. 52, 2197–2205. https://doi.org/10.1021/acs.est.7b05563.

Li, Y., Ma, S., Xu, S., Fu, H., Li, Z., Li, K., Sheng, K., Du, J., Lu, X., Li, X., Liu, S., 2020. Novel magnetic biochar as an activator for peroxymonosulfate to degrade bisphenol A: emphasizing the synergistic effect between graphitized structure and CoFe2O4. Chem. Eng. J., 124094. https://doi.org/10.1016/J.CEJ.2020.124094.

Liang, C., Bruell, C.J., 2008. Thermally activated persulfate oxidation of trichloroethylene: experimental investigation of reaction orders. Ind. Eng. Chem. Res. 47, 2912–2918. https://doi.org/10.1021/ie070820l.

Liang, C., Chen, Y.-J., Chang, K.-J., 2009. Evaluation of persulfate oxidative wet scrubber for removing BTEX gases. J. Hazard. Mater. 164, 571–579. https://doi.org/10.1016/J.JHAZMAT.2008.08.056.

Liang, P., Zhang, C., Duan, X., Sun, H., Liu, S., Tade, M.O., Wang, S., 2017. N-doped graphene from metal–organic frameworks for catalytic oxidation of p-Hydroxylbenzoic acid: N-Functionality and mechanism. ACS Sustain. Chem. Eng. 5, 2693–2701. https://doi.org/10.1021/acssuschemeng.6b03035.

Ma, Z., Yang, Y., Jiang, Y., Xi, B., Yang, T., Peng, X., Lian, X., Yan, K., Liu, H., 2017. Enhanced degradation of 2,4-dinitrotoluene in groundwater by persulfate activated using iron–carbon micro-electrolysis. Chem. Eng. J. https://doi.org/10.1016/j.cej.2016.11.083.

Makoś, P., Fernandes, A., Boczkaj, G., 2018. Method for the simultaneous determination of monoaromatic and polycyclic aromatic hydrocarbons in industrial effluents using dispersive liquid–liquid microextraction with gas chromatography–mass spectrometry. J. Sep. Sci. 41, 2360–2367. https://doi.org/10.1002/jssc.201701464.

Neppolian, B., Jung, H., Choi, H., Lee, J.H., Kang, J.-W., 2002. Sonolytic degradation of methyl tert-butyl ether: the role of coupled fenton process and persulphate ion. Water Res. 36, 4699–4708. https://doi.org/10.1016/S0043-1354(02)00211-7.

Oh, W.-D., Lua, S.-K., Dong, Z., Lim, T.-T., 2015. A novel three-dimensional spherical CuBi2O4 consisting of nanocolumn arrays with persulfate and peroxymonosulfate activation functionalities for 1H-benzotriazole removal. Nanoscale. 7, 8149–8158. https://doi.org/10.1039/C5NR01428J.

Oh, W.-D., Dong, Z., Lim, T.-T., 2016. Generation of sulfate radical through heterogeneous catalysis for organic contaminants removal: current development, challenges and prospects. Appl. Catal. B Environ. 194, 169–201. https://doi.org/10.1016/J.APCATB.2016.04.003.

Ouyang, D., Yan, J., Qian, L., Chen, Y., Han, L., Su, A., Zhang, W., Ni, H., Chen, M., 2017. Degradation of 1,4-dioxane by biochar supported nano magnetite particles activating persulfate. Chemosphere. 184, 609–617. https://doi.org/10.1016/j.chemosphere.2017.05.156.

Pawlowski Michael, H., 1998. Analytical and Field Test Methods for Measuring BTEX Metabolite Occurance and Transport in Groundwater.

Plata-Gryl, M., Jungnickel, C., Boczkaj, G., 2018. An improved scalable method of isolating asphaltenes. J. Pet. Sci. Eng. 167, 608–614. https://doi.org/10.1016/J.PETROL.2018.04.039.

Price, G.J., Clifton, A.A., 1996. Sonochemical acceleration of persulfate decomposition. Polymer (Guildf). 37, 3971–3973. https://doi.org/10.1016/0032-3861(96)00197-8.

Rastogi, A., Al-Abed, S.R., Dionysiou, D.D., 2009. Sulfate radical-based ferrous–peroxymonosulfate oxidative system for PCBs degradation in aqueous and sediment systems. Appl. Catal. B Environ. 85, 171–179. https://doi.org/10.1016/J.APCATB.2008.07.010.

Reddy, D.R., Dinesh, G.K., Anandan, S., Sivasankar, T., 2016. Sonophotocatalytic treatment of Naphthol Blue Black dye and real textile wastewater using synthesized Fe doped TiO2. Chem. Eng. Process. Process Intensif. 99, 10–18. https://doi.org/10.1016/J.CEP.2015.10.019.

Rong, X., Xie, M., Kong, L., Natarajan, V., Ma, L., Zhan, J., 2019. The magnetic biochar derived from banana peels as a persulfate activator for organic contaminants degradation. Chem. Eng. J. 372, 294–303. https://doi.org/10.1016/J.CEJ.2019.04.135.

Shukla, P., Sun, H., Wang, S., Ang, H.M., Tadé, M.O., 2011. Co-SBA-15 for heterogeneous oxidation of phenol with sulfate radical for wastewater treatment. Catal. Today 175, 380–385. https://doi.org/10.1016/J.CATTOD.2011.03.005.

Smith, M.R., 1990. The biodegradation of aromatic hydrocarbons by bacteria. Biodegradation. 1, 191–206. https://doi.org/10.1007/BF00058836.

Son, H.-S., Choi, S.-B., Khan, E., Zoh, K.-D., 2006. Removal of 1,4-dioxane from water using sonication: effect of adding oxidants on the degradation kinetics. Water Res. 40, 692–698. https://doi.org/10.1016/J.WATRES.2005.11.046.

Su, S., Guo, W., Yi, C., Leng, Y., Ma, Z., 2012. Degradation of amoxicillin in aqueous solution using sulphate radicals under ultrasound irradiation. Ultrason. Sonochem. 19, 469–474. https://doi.org/10.1016/J.ULTSONCH.2011.10.005.

Sun, H., Liu, S., Zhou, G., Ang, H.M., Tadé, M.O., Wang, S., 2012. Reduced graphene oxide for catalytic oxidation of aqueous organic pollutants. ACS Appl. Mater. Interfaces 4, 5466–5471. https://doi.org/10.1021/am301372d.

Wacławek, S., Lutze, H.V., Grübel, K., Padil, V.V.T., Černík, M., Dionysiou, D.D., 2017. Chemistry of persulfates in water and wastewater treatment: a review. Chem. Eng. J. https://doi.org/10.1016/j.cej.2017.07.132.

Wacławek, S., Padil, V.V.T., Černík, M., 2018. Major advances and challenges in heterogeneous catalysis for environmental applications: a review. Ecol. Chem. Eng. S. 25, 9–34. https://doi.org/10.1515/eces-2018-0001.

Wang, S., Zhou, N., Wu, S., Zhang, Q., Yang, Z., 2015. Modeling the oxidation kinetics of sono-activated persulfate's process on the degradation of humic acid. Ultrason. Sonochem. 23, 128–134. https://doi.org/10.1016/J.ULTSONCH.2014.10.026.

Wang, Y., Cao, D., Liu, M., Zhao, X., 2017. Insights into heterogeneous catalytic activation of peroxymonosulfate by Pd/g-C3N4: the role of superoxide radical and singlet oxygen. Catal. Commun. 102, 85–88. https://doi.org/10.1016/J.CATCOM.2017.08.016.

Wang, S., Zhou, N., 2016. Removal of carbamazepine from aqueous solution using sono-activated persulfate process. Ultrason. Sonochem. 29, 156–162. https://doi.org/10.1016/J.ULTSONCH.2015.09.008.

Yadav, J.S., Reddy, C.A., 1993. Degradation of benzene, toluene, ethylbenzene, and xylenes (BTEX) by the lignin-degrading basidiomycete Phanerochaete chrysosporium. Appl. Environ. Microbiol. 59, 756–762.

Yin, R., Guo, W., Wang, H., Du, J., Zhou, X., Wu, Q., Zheng, H., Chang, J., Ren, N., 2018. Enhanced peroxymonosulfate activation for sulfamethazine degradation by ultrasound irradiation: performances and mechanisms. Chem. Eng. J. 335, 145–153. https://doi.org/10.1016/J.CEJ.2017.10.063.